Study of $T=\frac{3}{2}$ states in $^{17}F^{\dagger}$

B. M. Skwiersky,* C. M. Baglin, and P. D. Parker
Wright Nuclear Structure Laboratory, Yale University, New Haven, Connecticut 06520
(Received 10 September 1973)

The first seven $T=\frac{3}{2}$ states in ^{17}F have been studied as resonances in the $^{16}O+p$ entrance channel, observing the (p_0), (p_1+p_2), (p_3+p_4), and (α_0) exit channels. In a survey of the energy region $E_p=13.23$ to 16.60 MeV in steps of less than 5 keV at six laboratory angles, the previously unobserved fourth and fifth $T=\frac{3}{2}$ states were found at $E_p=13.271\pm0.004$ and 14.017 ± 0.004 MeV, respectively. Complete elastic scattering angular distributions (at 29 angles from $\theta_{lab}=25$ to 165°) were measured from $E_p=9.0$ to 20.35 MeV in 50-keV steps and were analyzed using the optical-model code JIB3 to extract phase-shift information across this region. These results were used in a phase-shift analysis of the individual $T=\frac{3}{2}$ resonances to obtain the following assignments for the second through the seventh $T=\frac{3}{2}$ states in ^{17}F:

E_p (MeV)	$E_x(^{17}F)$ (MeV)	Γ (keV)	Γ_{p_0}/Γ	J^{π}
12.708 ± 0.004	12.551	3 ± 1	0.26 ± 0.04	$\frac{3}{2}^-$
13.250 ± 0.004	13.061	2 ± 1	0.15 ± 0.04	$\frac{5}{2}^-$
13.271 ± 0.004	13.080	2 ± 1	0.04 ± 0.02	$(\frac{1}{2}^+)$
14.017 ± 0.004	13.782	12 ± 5	0.02 ± 0.01	$\frac{5}{2}^+$
14.438 ± 0.006	14.177	27 ± 5	0.04 ± 0.02	$\frac{3}{2}^-$
14.579 ± 0.010	14.310	20 ± 5	0.11 ± 0.03	$\frac{7}{2}^-$

[NUCLEAR REACTIONS $^{16}O(p,p)$, (p,α) $E=9.0$–20.4 MeV; measured $\sigma(E;\theta)$; deduced optical-model parameters. Phase-shift analysis; $^{17}F(T=\frac{3}{2})$ levels as compound-nucleus resonances; deduced E_x, Γ, Γ_{p_0}/Γ, J^{π}.]

I. INTRODUCTION

The precise location of at least four members of an isospin multiplet is necessary for any test of the quadratic mass law, and such tests have been carried out for the ground-state analogs in a number of quartets.[1] If such tests can be carried out for excited-state analogs in the same multiplet, it is then possible to study the coefficients of the mass law as functions of nuclear configurations and to examine isospin purity and isospin mixing as functions of excitation energy in the multiplet.

The $A=17$, $T=\frac{3}{2}$ quartet has been studied for nearly 10 years, and during that time a large number of $T=\frac{3}{2}$ states have been located in the various members of the multiplet, as recently reviewed by Ajzenberg-Selove.[2] Although the present accuracy of the ^{17}Ne data[3] is not sufficient to permit a significant test of the validity of the quadratic form of the mass law in this multiplet, the accurate energies of the $T_z=\frac{3}{2}, \frac{1}{2}$, and $-\frac{1}{2}$ projections in the quartet can still be used to make a comparison of the mass-law coefficients for various $T=\frac{3}{2}$ levels within the $A=17$ multiplet. It must be cautioned, however, that as the energy separation of excited $T=\frac{3}{2}$ states decreases it becomes necessary to identify the levels under comparison by signatures other than just their energies. Until we have a better understanding of the ways in

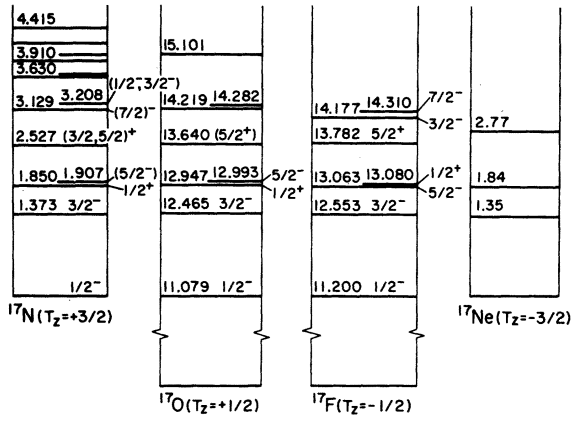

FIG. 1. $T=\frac{3}{2}$ energy levels in the $A=17$ quartet. Excitation energies and J^{π} assignments are compiled from Refs. 2, 3, 5–8, and the results of the experiments presented in this paper. Relative to the ^{17}F ground state the $^{16}O+p$ entrance channel has a positive Q value of 0.601 MeV, and the allowed $T=\frac{3}{2}$ exit channels lie at 12.726 MeV ($^{15}N+2p$) and at 13.396, 13.568, 13.694, and 13.859 MeV [^{16}O $(T=1)+p$].

which the decays and other dynamic properties of these states vary from one isospin projection to another, this identification will normally require spin and parity information. For this reason, and in view of the success of LeVine and Parker[4] in the phase-shift analysis of the $T=\frac{3}{2}$ levels in ^{13}N seen as resonances in the $^{12}C+p$ entrance channel, we have extended their work to the $A=17$ system in order to locate a number of missing $T=\frac{3}{2}$, $T_z=-\frac{1}{2}$ analog states and to study the $T=\frac{3}{2}$ states in ^{17}F as resonances in the $^{16}O+p$ entrance channel in order to extract spin and parity information.

Figure 1 summarizes the present knowledge of the $T=\frac{3}{2}$ level structure in the $A=17$ quartet, including the data compiled in Ref. 2, the results of the present experiments, and the results of other recent studies by Hartwig[5] [the $^{18}O(d,{}^3He)^{17}N$ reaction], by McDonald *et al.*[6] [the $^{13}C(\alpha,n)^{16}O$ reaction], by Harakeh, Snover, and Paul[7] [the $^{16}O(p,\gamma)^{17}F$ reaction], and by Becker *et al.*[8] [the $^{11}B(^7Li,p)^{17}N$ reaction].

II. EXPERIMENTAL PROCEDURE

Proton beams in the energy range 6.0 to 20.35 MeV were obtained from the Yale MP tandem Van de Graaff accelerator. The energy calibration of its analyzing magnet system[9] allowed the determination of resonance energies to within ±4 keV. As a check on the magnet calibration, the lowest ^{13}N $T=\frac{3}{2}$ resonance, observed in the $^{12}C(p,p)$ reaction at $E_p=14.231\pm0.004$ MeV by Levine and Parker,[4] was located at the start of each period of accelerator beam time. A 76-cm ORTEC scattering chamber (equipped with two externally mounted 0.16-cm-diam entrance apertures 76 cm apart and a 0.48-cm-diam antiscattering aperture at the end of a snout extending 25.4 cm into the scattering chamber's interior) was used through-

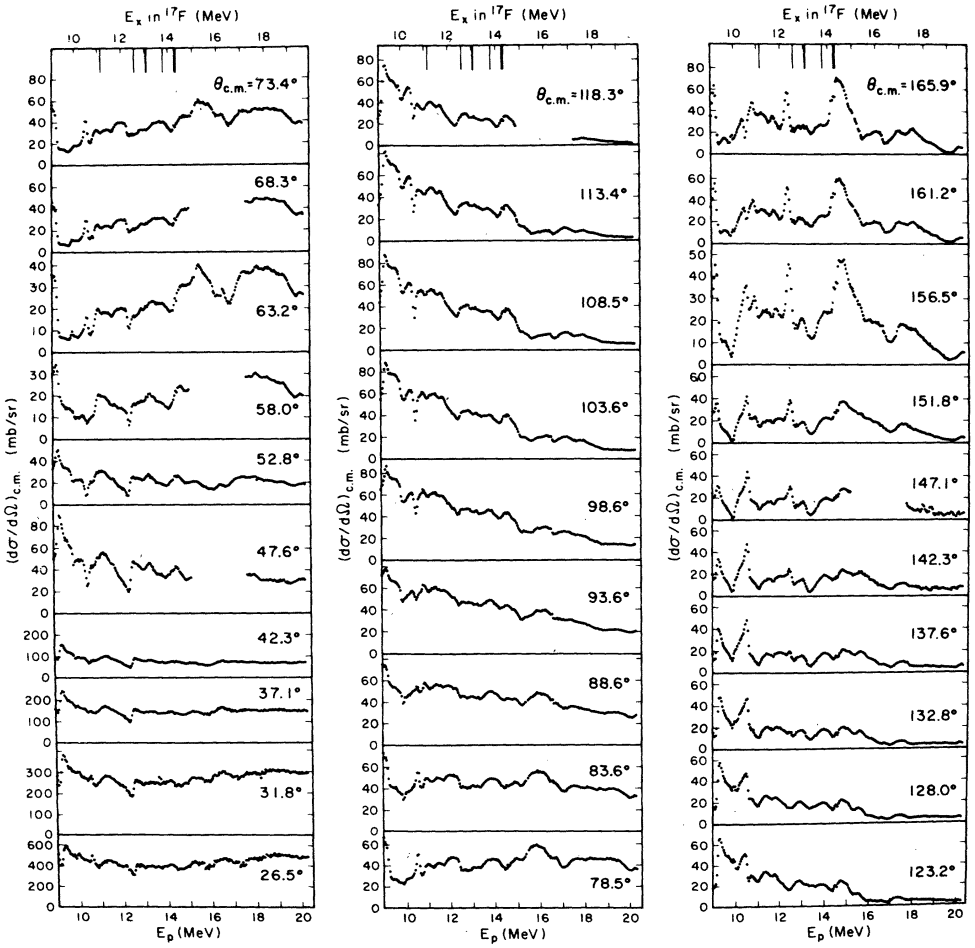

FIG. 2. $^{16}O(p,p)^{16}O$ elastic scattering excitation functions measured in 50-keV steps from 9.00 to 20.35 MeV. The lines at the top of each graph indicate the locations of the $T=\frac{3}{2}$ states in ^{17}F studied in our experiments.

out the course of the experiment. To ensure proper charge integration, an annular magnet, with its field along a diameter, was placed at the entrance to the Faraday cup.

For the high-resolution data required for the location and study of the $T=\frac{3}{2}$ states, ^{7}LiO targets (typically 80 μg/cm^2 thick) were used primarily because the additional elastic and inelastic peaks from the ^{7}Li interfered less with our measurements than in the case of other chemical compounds which we tried, e.g. SiO. (The ^{7}LiO targets were prepared by evaporating ^{7}Li onto 10-μg/cm^2 carbon foils and then exposing these targets to a dry oxygen atmosphere.) The energy losses and straggling associated with the windows of a gas cell precluded the use of gaseous oxygen as a target for the study of the narrow resonances frequently associated with isobaric analog states, but a gas cell was used in the survey of ^{16}O(p,p)-^{16}O elastic scattering at 29 angles ($26.5^\circ \leq \theta_{\text{c.m.}} \leq 165.9^\circ$) in 50-keV steps from $E_p = 9.00$ to 20.35 MeV, e.g. Fig. 2. (A tabulation of these cross sections is available from the authors.) The window of the cell was 2-mg/cm^2-thick Havar[10]; the gas pressure (typically 40 cm of Hg) was monitored with a mercury manometer and never varied by more than $\pm 0.5\%$ in 24 hours. During the two-week run the gas was changed every day or two to reduce the accumulation of impurities in the gas which might result from any outgassing of the cell.

Transmission-mounted, Si(SB) detectors were used to detect the protons and α particles. Small, diametrically magnetized annular magnets were placed in front of each detector assembly to prevent secondary electrons from reaching the detectors. Signal handling was performed using standard NIM modules, and processed data were routed either into a multichannel analyzer or through a number of single-channel-analyzer (SCA) windows (set on appropriate peaks in the spectra) into a corresponding group of scalers. For most of the resonances studied the exit channels p_0, p_1+p_2 ($Q=-6.05$ and -6.13 MeV), p_3+p_4 ($Q=-6.92$ and -7.12 MeV), and α_0 ($Q=-5.22$ MeV) were monitored at every angle at which the associated peaks were well resolved in the spectrum. In some of the inelastic and (p,α_0) data the presence of a significant background within the SCA window prevented the extraction of true cross sections, but still permitted a qualitative study of the effect of the resonances on these channels.

For the elastic scattering measurements using the gas target, absolute cross sections were obtained with uncertainties of $\lesssim 5\%$; $\lesssim 3\%$ from counting statistics, $\lesssim 1\%$ from the charge integration (checked with a calibrated current source), $\lesssim 1\%$ from the gas pressure (measured with a mercury namometer), and $\lesssim 3\%$ from the measurement of the detector G factors using Rutherford scattering from xenon gas at $E_p = 6.00$ MeV. Cross sections for the LiO target measurements were obtained from normalizations to the gas target results.

III. ANALYSIS

Preliminary identification of $T > |T_z|$ analog states in a T_z nucleus is often made solely on the basis of an excitation energy which is in approximate agreement with the predictions of Coulomb displacement calculations. Supporting evidence can sometimes be obtained from a study of the isospin-allowed vs isospin-forbidden decay modes for such a state and from a study of the relative population of the state via isospin-allowed and -forbidden reactions. However, because such Coulomb energy calculations are never exact and because of the frequent admixtures of isospin impurities into analog states, all such evidence should only be viewed as qualitative.

More quantitative evidence can be obtained from a comparison of the angular distributions of reactions leading to the various T_z projections of the state[11] or from a determination of the spin and parity of the state in comparison with the spin and parity of the parent state in the $T_z = \pm T$ nucleus. To obtain the spin and parity information for the $T=\frac{3}{2}$ analog states in ^{17}F we have undertaken a phase-shift analysis of resonances seen in ^{16}O$+p$ elastic scattering data.

For a spin-$\frac{1}{2}$ projectile colliding elastically with a spin-0 target, the differential cross section can be expressed as[12]

$$\frac{d\sigma}{d\Omega} = |A|^2 + |B|^2, \tag{1}$$

where

$$A = f_c(\theta) + \frac{1}{2ik}\sum_{l=0}^{\infty} \exp[2i(\omega_l - \omega_0)]\{(l+1)[\exp(2i\delta_l^+)-1] + l[\exp(2i\delta_l^-)-1]\} P_l(\theta),$$

$$B = \frac{1}{2ik}\sum_{l=1}^{\infty} \exp[2i(\omega_l - \omega_0)]\{\exp(2i\delta_l^+) - \exp(2i\delta_l^-)\} P_l^1(\theta);$$

and where

$$f_c(\theta) = -[\eta/2k\sin^2(\theta/2)]\exp\{-i\eta\ln[\sin^2(\theta/2)]\};$$

$\eta = (zZe^2/\hbar v)$; $k = mv/\hbar$; θ is the scattering angle; v the relative velocity; ω_l the lth Coulomb phase shift; and $\delta_l^{\pm}$ the scattering phase shift corresponding to the $j = l \pm \frac{1}{2}$ partial wave.

Because the $T=\frac{3}{2}$ states in ^{17}F lie at high excitation energies, many exit channels are energetically available to the compound nucleus. In order to include the effects of these open reaction channels in the elastic scattering analysis, complex phase shifts ($\delta_l^{\pm}$) were used, and the collision matrix elements were rewritten as

$$\begin{aligned} U_l^{\pm} &= \exp(2i\delta_l^{\pm}) \\ &= A_l^{\pm}\exp(2i\Delta_l^{\pm}), \end{aligned} \tag{2}$$

where both $A_l^{\pm}$ and $\Delta_l^{\pm}$ are real and where $0 \leq A_l^{\pm} \leq 1$.

For a resonant partial wave the usual dispersion term is added to the appropriate collision matrix element:

$$\begin{aligned} U_l^{\pm} &= \exp(2i\Delta_l^{0\pm})\left[A_l^{0\pm} - \frac{\Gamma_0 e^{i\gamma}}{E - E_0 + \frac{1}{2}i\Gamma}\right] \\ &= \exp(2i\Delta_l^{0\pm})\left[A_l^{0\pm} + \frac{\Gamma_0 e^{i\gamma}e^{i\beta}}{[(E-E_0)^2 + \frac{1}{4}\Gamma^2]^{1/2}}\right], \end{aligned} \tag{3}$$

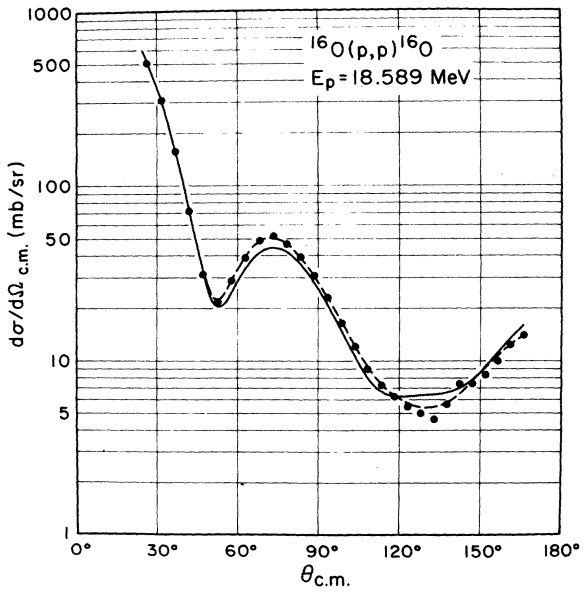

FIG. 3. A typical angular distribution for ^{16}O(p,p)^{16}O elastic scattering. The two curves are optical-model fits to the data obtained using the code JIB3 (Refs. 13, 14); the comparison between the solid and dashed lines is discussed in the text. The relative error bars on the points are $\leq 4\%$ and are smaller than the points.

where $\beta = \tan^{-1}[\frac{1}{2}\Gamma(E_0 - E)]$, where Γ_0 and Γ are the elastic scattering partial width and the total width, respectively, where $A_l^{0\pm}$ and $\Delta_l^{0\pm}$ are the off-resonance phase-shift amplitude and angle for $j = l \pm \frac{1}{2}$, and where γ is an arbitrary phase subject to the unitarity restriction that $|U_l^{\pm}| \leq 1$.

The problem of determining the off-resonance parameters $A_l^{0\pm}$ and $\Delta_l^{0\pm}$ at high excitation energies in the presence of a large number of broad and overlapping states was handled using an optical-model parametrization.[4] The elastic scattering angular distributions (e.g. Fig. 3) measured in 50-keV steps from $E_p = 9.00$ to 20.35 MeV were analyzed using the code JIB3, written by Perey and modified by Siemssen.[13,14] The optical-model potential used for this analysis has the form

$$\begin{aligned} V_{\rm opt} &= -V_R f(r, r_R, a_R) + 4ia_I W_S \frac{d}{dr} f(r, r_I, a_I) \\ &\quad + \vec{\sigma}\cdot\vec{l}\, V_{so}(\hbar/m_\pi c)^2 \frac{1}{r_{so}A^{1/3}} \frac{d}{dr} f(r, r_{so}, a_{so}) \\ &\quad + V_{\rm Coul}(r, r_c), \end{aligned} \tag{4}$$

where

$$f(r, r_0, a_0) = 1/\{1 + \exp[(r - r_0A^{1/3})/a_0]\},$$

and where

$$\begin{aligned} V_{\rm Coul} &= \frac{zZe^2}{2R_c}[3 - (r/R_c)^2] \quad \text{for } r \leq R_c = r_cA^{1/3} \\ &= (zZe^2/r) \quad \text{for } r > R_c. \end{aligned}$$

For the present analysis we restricted the optical-model search to a fixed geometry, $r_R = r_I = r_{so} = r_c = 1.25$ fm, $a_R = a_{so} = 0.57$ fm, and $a_I = 0.50$ fm. With this fixed geometry, and using the parameters of Watson, Singh, and Segal[14] as starting values, the depths of the potentials were allowed to vary freely and are plotted as functions of proton energy in Fig. 4. These well parameters were then converted into an energy-dependent set of complex phase-shift parameters $A_l^{0\pm}$ and $\Delta_l^{0\pm}$ which are plotted as functions of proton energy in Fig. 5. The $l=4$ phases were small; e.g. at 18 MeV $\Delta_4^{0+} = 9°$, $A_4^{0+} = 0.90$, and $\Delta_4^{0-} = 4°$, $A_4^{0-} = 0.94$. For higher l waves these parameters were even less significant; $\Delta_l^{0\pm} < 1°$ and $A_l^{0\pm} > 0.99$.

A comparison of the two curves in Fig. 3 shows the effect of allowing the well geometries to vary after the well depths are determined. The resulting fits (solid line—fixed geometry, only well depths varied; dashed line—well geometries varied after the well depths were determined) are not qualitatively different, and the only significant change in the resulting phase shifts is a 20 to 25° reduction in the f-wave phases, Δ_3^- and Δ_3^+, and a reduction of A_3^- from 0.36 to 0.11. Changes in the other $\Delta_l^{\pm}$ are $\lesssim 3°$ and in the other $A_l^{\pm}$ are only a

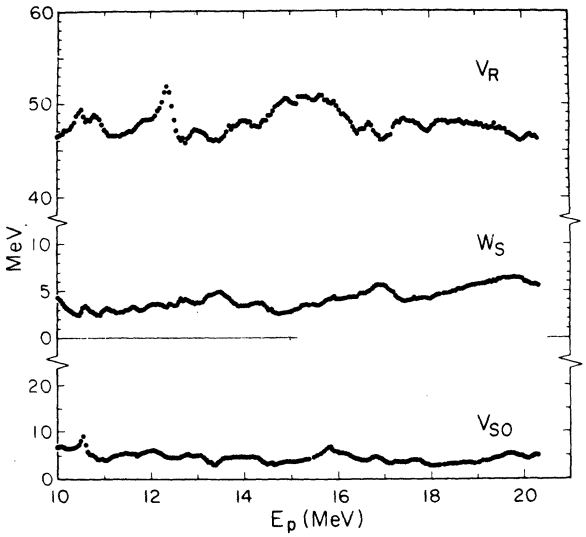

FIG. 4. Energy dependence of the optical-model well depths for the case where the geometries of the potential wells were fixed at $r_R = r_I = r_{so} = r_c = 1.25$ fm, $a_R = a_{so} = 0.57$ fm, and $a_I = 0.50$ fm.

few percent.

The evaluation and interpretation of such a multiparameter analysis is always an extremely subjective process; the choices of starting values and variation parameters introduce a strong bias justifiable only in terms of accomodation to previous or related work[14-16] and to self-consistency. The phase shifts of Hardie, Dangle, and Oppliger[16] are compared with the present results in Fig. 5 and show generally good agreement in the region of overlapping energies.

Further confidence in this analysis is provided by our use of the resulting phase shifts to extract spin and parity assignments for levels where these assignments had been previously established. In all of the cases presented in this paper, the phase-shift analysis was carried out by fixing the phase shifts for all but one of the partial waves at the values extracted from the optical-model analysis and requiring that the energy dependence for the resonant partial wave be given by the dispersion term in Eq. (3). Differential cross sections generated in this way (including the effects of finite beam resolution, $\Delta E = 2$ keV) were then compared to the elastic scattering excitation functions at the specific angles to determine which partial wave was resonating and to determine its resonance parameters. Figure 6 shows the results of such an analysis for the second $T = \frac{3}{2}$ state in ^{17}F using the data of Hardie, Dangle, and Oppliger[16] ($J^\pi = \frac{3}{2}^-$, $T = \frac{3}{2}$, $\Gamma = 3$ keV, $\Gamma_{p_0}/\Gamma = 0.26$, and $\gamma = 130°$). (The Wisconsin data[16] have been shifted by $+37 \pm 5$ keV to compensate for their energy reproducibility problems[17] and to correct their ener-

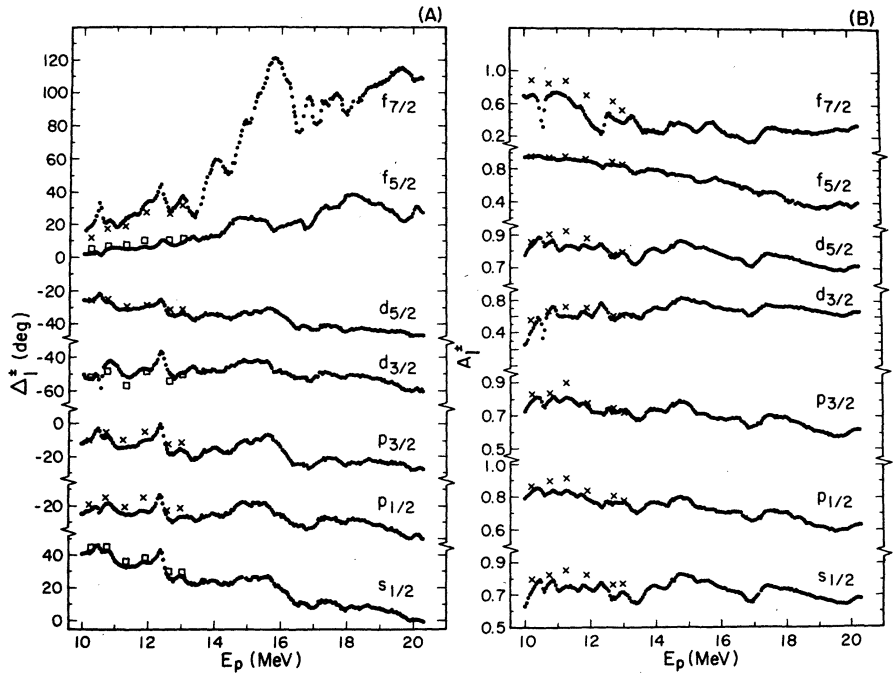

FIG. 5. Energy dependence of the complex phase-shift parameters, $\Delta_l^\pm$ and $A_l^\pm$, corresponding to the optical-model parameters in Fig. 4. The complex phase-shift solutions of Hardies, Dangle, and Oppliger (Ref. 16) are plotted as ×'s and □'s.

gy calibration to bring their data into agreement with our measurements of the location of this resonance. See also footnote 42 in Ref. 18.) Such an analysis also produced good agreement with the data for the resonance at $E_p = 12.450 \pm 0.020$ MeV ($J^\pi = \frac{3}{2}^-$, $T = \frac{1}{2}$, $E_x = 12.309$ MeV, $\Gamma = 200 \pm 50$ keV, $\Gamma_{p_0}/\Gamma = 0.4 \pm 0.2$, and $\gamma = 90°$). (In Ref. 2 this resonance is listed at $E_p = 12.39$ MeV, but must also be shifted because of the calibration problem noted above.) The agreement between the results of these analyses and the previously accepted values for these levels[2] serves as a check both on the optical-model analysis and on our phase-shift analysis procedures and programs.

IV. RESULTS

$E = 11.200$ MeV ($T = \frac{3}{2}$ ground state); proton decay

In 1969, in a preliminary analysis of the delayed-proton emitter ^{17}Ne, Hardy, Esterl, Sextro, and Cerny[19] reported a substantial ($26 \pm 8\%$) decay from the lowest $T = \frac{3}{2}$ state in ^{17}F to the 0^+, 6.05-MeV state in ^{16}O with no decay (<10%) observed to the 3^-, 6.13-MeV state in ^{16}O. This result was in disagreement with the earlier results of Patterson, Winkler, and Zaidins[20] which suggested that the dominant decay modes for this state were proton emission to the 6.13- and 7.12-MeV states in ^{16}O. During the course of our measurements, a careful study of the various elastic, inelastic, and reaction channels in the neighborhood of this resonance indicated $\Gamma_{p_2} \gg \Gamma_{p_1}$, in good agreement with the results of Patterson, Winkler, and Zaidins.[20] At $\theta_{lab} = 165°$ the p_1 group has less than 5% of the intensity of the p_2 group and shows a variation of <20% in its intensity at the resonance compared to the 10% variation in the intensity of the p_2 group. More recently, the final analysis of the ^{17}Ne delayed-proton data by Hardy *et al.*[18] (see particularly their footnote 47 and their Table VI) is now consistent with the ^{16}O(p, p') results, indicating a ratio for the decays of this state to the 6.05- and 6.13-MeV states in ^{16}O of $\nu(6.13)/\nu(6.05) > 20$ when penetration effects are included.

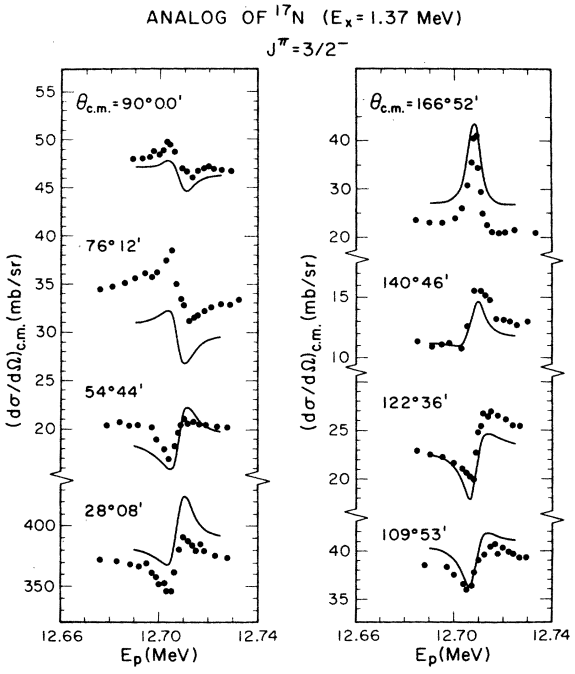

FIG. 6. Phase-shift analysis of the ^{16}O$(p,p)^{16}$O elastic scattering data for the $T = \frac{3}{2}$ resonance at $E_p = 12.71$ MeV. The data are taken from the work of Hardie, Dangle, and Oppliger (Ref. 16) and have been shifted slightly in energy as discussed in the text.

$E = 12.553$ MeV ($T = \frac{3}{2}$ first excited state)

In view of the extensive elastic scattering data already published for this resonance,[16,20,21] we used this resonance ($E_p = 12.708 \pm 0.004$ MeV) only as a check on our energy resolution, and as a check of our analysis procedures, as already described above (see Fig. 6). The resulting parameters extracted by our analysis of the Wisconsin data[16] for this resonance are listed in Table I.

$E = 13.063/13.080$ MeV ($T = \frac{3}{2}$ second and third excited states)

The $T_z = \frac{1}{2}$ analogs of the 1.85-MeV ($\frac{1}{2}^+$) and 1.91-MeV ($\frac{5}{2}^-$) states in ^{17}N are found in ^{17}O at 12.947 MeV ($\frac{1}{2}^+$) and 12.993 MeV ($\frac{5}{2}^-$); see Fig. 1. In ^{17}F, Hardie, Dangle, and Opplinger[16] found a narrow resonance in this region and noted that there was a suggestion of a doublet in the structure they observed. Van Bree and Temmer[21] also studied this region very carefully using the ^{16}O(p, p_0) and (p, p') reactions but were able to extract only one resonance ($E_x = 13.066 \pm 0.008$ MeV) from their data for which they derived an assignment of $\frac{5}{2}^-$ or $\frac{7}{2}^-$. The ^{19}F$(p, t)^{17}$F reaction populates one level in this region very strongly[22,23] (presumably the $\frac{1}{2}^+$ analog) but the energy resolution (~50 to 100 keV) was not sufficient to locate the state accurately or to resolve the two states if both were populated. The ^{15}N$(^3$He$, n)^{17}$F reaction was observed[24,25] to populate one level in this region ($E_x = 13.059 \pm 0.009$ MeV, $\Gamma < 25$ keV) for which a tentative assignment of $\frac{3}{2}^-$ or $\frac{5}{2}^-$ was made.[25] More recently, Harakeh, Snover, and Paul[7] observed a narrow resonance in the ^{16}O$(p, \gamma_0)^{17}$F reaction corresponding to $E_x = 13.065 \pm 0.006$ MeV ($\Gamma \leq 8$ keV). The predominantly $E1$ character of the γ decay indicates an assignment of $\frac{3}{2}^-$, $\frac{5}{2}^-$, or

$\frac{7}{2}^-$ for this level.

Our data in this energy region are presented in Figs. 7 and 8. In addition to the strong resonance at $E_p = 13.250 \pm 0.004$ MeV ($E_x = 13.061 \pm 0.004$ MeV, $\Gamma = 2 \pm 1$ keV), there is also clear evidence (for example, in the elastic scattering data at $\theta_{c.m.} = 137.6$ and $166.0°$) for the second member of the $T = \frac{3}{2}$ doublet at $E_p = 13.271 \pm 0.004$ MeV ($E_x = 13.080 \pm 0.004$ MeV, $\Gamma = 2 \pm 1$ keV). A single-level phase-shift analysis was carried out for each of the members of this doublet with the phase-shift parameters for the nonresonant partial waves fixed at the values extracted from the optical-model analysis described above and with the resonant partial wave required to have the dispersion form of Eq. (3). In the case of the lower member of this doublet ($E_p = 13.250$ MeV), only the $\frac{5}{2}^-$ partial wave could produce a reasonable prediction of the shapes of the experimental excitation functions. For the upper member of this doublet ($E_p = 13.271$ MeV) the effect of the resonance is too weak in the elastic scattering to be decisive in determining the resonant partial wave. The curve through the data in Fig. 7 at the upper resonance shows that a consistent description of the data can be obtained for a $J^\pi = \frac{1}{2}^+$ assignment, compatible with the $^{19}F(p,t)^{17}F$ results[22,23] and with the assignments in ^{17}N and ^{17}O. The resulting resonance parameters are listed in Table I. The errors assigned are subjective estimates of how

TABLE I. Properties of $T = \frac{3}{2}$ levels in $A = 17$.

E_x (^{17}N) [a] (MeV)	E_x (^{17}O) [b] (MeV)	E_x (^{17}F) (MeV)	Reaction	E_p (MeV)	Γ (keV)	Γ_{p_0}/Γ	J^π	γ [c] (deg)	Ref.
0.00	11.079 ± 0.005	11.06 ± 0.03	$^{19}F(p,t)^{17}F$	···			$(\frac{1}{2}^-, \frac{3}{2}^-)$		d
		11.195 ± 0.007	$^{15}N(^3He,n)^{17}F$	···	<20		$\frac{1}{2}^-$		e
		11.202 ± 0.008	$^{16}O(p,p)^{16}O$	11.276	<0.8	0.20	$\frac{1}{2}^-$		f
		11.196 ± 0.007	$^{16}O(p,p)^{16}O$	11.266	0.5	0.10	$\frac{1}{2}^-, \frac{3}{2}^-$		g
		11.204 ± 0.006	$^{16}O(p,\gamma)^{17}F$	11.275	≤3	0.088 ± 0.016	$\frac{1}{2}^-$		h
1.373 ± 0.001	12.465 ± 0.004	12.53 ± 0.03	$^{19}F(p,t)^{17}F$	···			$(\frac{1}{2}^-, \frac{3}{2}^-)$		d
		12.540 ± 0.008	$^{15}N(^3He,n)^{17}F$	···	<25		$\frac{3}{2}^-, \frac{5}{2}^-$		e
		12.554 ± 0.008	$^{16}O(p,p)^{16}O$	12.714	<3.3		$\frac{3}{2}^-$		f
		12.556 ± 0.007	$^{16}O(p,p)^{16}O$	12.713	1.8	0.30	$\frac{3}{2}^-$		g
		12.553 ± 0.006	$^{16}O(p,\gamma)^{17}F$	12.710	<3				h
		12.551 ± 0.004	$^{16}O(p,p)^{16}O$	12.708	3 ± 1	0.26 ± 0.04	$\frac{3}{2}^-$	130	i
1.850 ± 0.001	12.947 ± 0.006	13.02 ± 0.04	$^{19}F(p,t)^{17}F$	···			$(\frac{1}{2}^+)$		d
		13.080 ± 0.004	$^{16}O(p,p)^{16}O$	13.271	2 ± 1	0.04 ± 0.02	$(\frac{1}{2}^+)$	10	j
1.907 ± 0.001	12.993 ± 0.006	13.059 ± 0.009	$^{15}N(^3He,n)^{17}F$	···	<25		$(\frac{3}{2}^-, \frac{5}{2}^-)$		e
		13.065 ± 0.007	$^{16}O(p,p)^{16}O$	13.255	≤2	0.19	$\frac{5}{2}^-, \frac{7}{2}^-$		g
		13.065 ± 0.006	$^{16}O(p,\gamma)^{17}F$	13.255	≤8	0.20			h
		13.061 ± 0.004	$^{16}O(p,p)^{16}O$	13.250	2 ± 1	0.15 ± 0.04	$\frac{5}{2}^-$	160	j
2.527 ± 0.001	13.640 ± 0.005	13.782 ± 0.004	$^{16}O(p,p)^{16}O$	14.017	12 ± 5	0.02 ± 0.01	$\frac{5}{2}^+$	0	j
3.129 ± 0.001	(14.282 ± 0.006)	14.311 ± 0.012	$^{16}O(p,p)^{16}O$	14.580	<20	0.17	$(\ )^-$		g
		14.309 ± 0.006	$^{16}O(p,\gamma)^{17}F$	14.578	34 ± 5	0.17	$(\frac{3}{2}, \frac{5}{2}, \frac{7}{2})^-$		h
		14.310 ± 0.010	$^{16}O(p,p)^{16}O$	14.579	20 ± 5	0.11 ± 0.03	$\frac{7}{2}^-$	115	j
3.208 ± 0.002	(14.219 ± 0.008)	14.179 ± 0.012	$^{16}O(p,p)^{16}O$	14.440	≤50		$(\ )^-$		g
		14.174 ± 0.010	$^{16}O(p,\gamma)^{17}F$	14.434	42 ± 10		$(\frac{3}{2}, \frac{5}{2}, \frac{7}{2})^-$		h
		14.177 ± 0.006	$^{16}O(p,p)^{16}O$	14.438	27 ± 5	0.04 ± 0.02	$\frac{3}{2}^-$	180	j

[a] References 2 and 8.
[b] References 2 and 6.
[c] The phase angle γ is defined in the text.
[d] Reference 22.
[e] References 24 and 25.
[f] Reference 20.
[g] Reference 21.
[h] Reference 7.
[i] Reference 16 and present analysis.
[j] Present results.

much a given parameter could vary before the quality of the comparisons deteriorated significantly and the fits became unreasonable.

In Fig. 7, it is clear that there are problems in the magnitude of the absolute cross sections predicted at 137.6 and 151.8°. These could be improved considerably by changes in the nonresonant phases, but we feel that there is less significance in such multiparameter variational games and their results than in the comparison presented here. In addition to the choice of resonant partial wave and the position (E_0) and width (Γ) of the resonance, there were *only* two free parameters at each resonance [(Γ_{p_0} the elastic scattering partial width, and γ the relative phase defined in Eq. (3)] which could be used to obtain these fits.

$E=13.782$ MeV ($T=\frac{3}{2}$ fourth excited state)

This state had not been previously observed in ^{17}F. In the present data (e.g. Figs. 9 and 10) it is seen prominently in the (p, α_0) and (p, p') channels but only weakly in the elastic scattering ($\Gamma_{p_0}/\Gamma = 0.02 \pm 0.01$). A phase-shift analysis, using the procedures discussed above, establishes $J^\pi = \frac{5}{2}^+$. A comparison of the resulting cross-section predictions with the experimental excitation functions is shown in Fig. 9. The resonance parameters extracted from this analysis are listed in Table I.

Our assignment of $\frac{5}{2}^+$ to this level is consistent (1) with the tentative assignment of $\frac{5}{2}^+$ to the $T_z=\frac{1}{2}$ analog in ^{17}O by Détraz and Duhm[26] on the basis

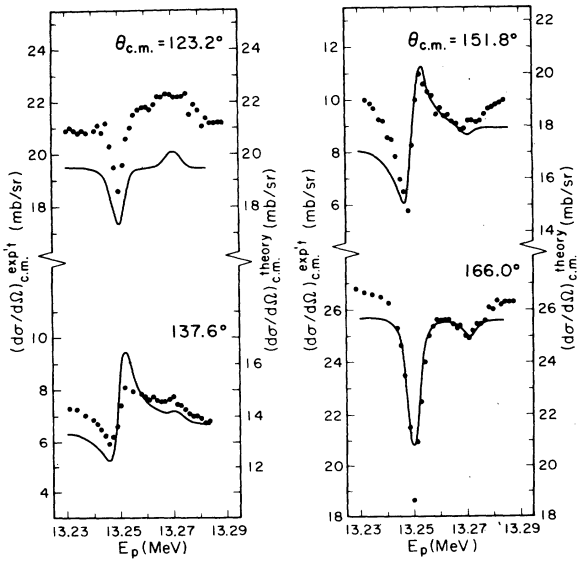

FIG. 7. Single-level phase-shift analyses of the ^{16}O-(p,p)^{16}O elastic scattering data for the $T=\frac{3}{2}$ resonances at $E_p=13.25$ and 13.27 MeV.

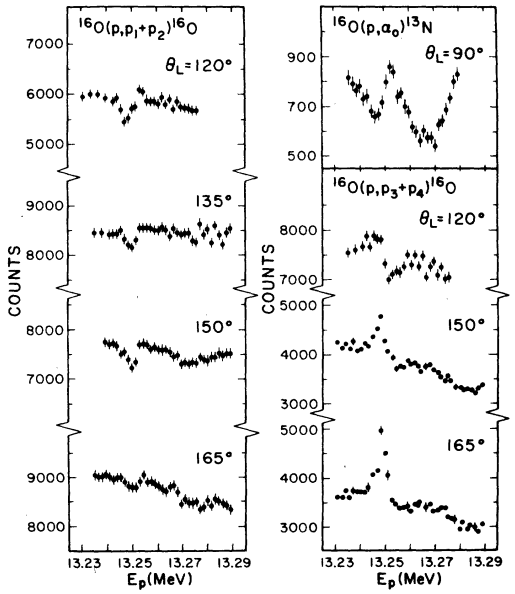

FIG. 8. ^{16}O(p,p')^{16}O and ^{17}O(p,α)^{13}N data at the $T=\frac{3}{2}$ resonances at $E_p=13.25$ and 13.27 MeV. Sample relative error bars are shown.

of a distorted-wave Born-approximation (DWBA) analysis of ^{18}O(^{3}He, α)^{17}O data; (2) with a more recent assignment[5,8] of $(\frac{3}{2}, \frac{5}{2})^+$ to the $T_z=\frac{3}{2}$ member in ^{17}N; and (3) with the failure of Harakeh,

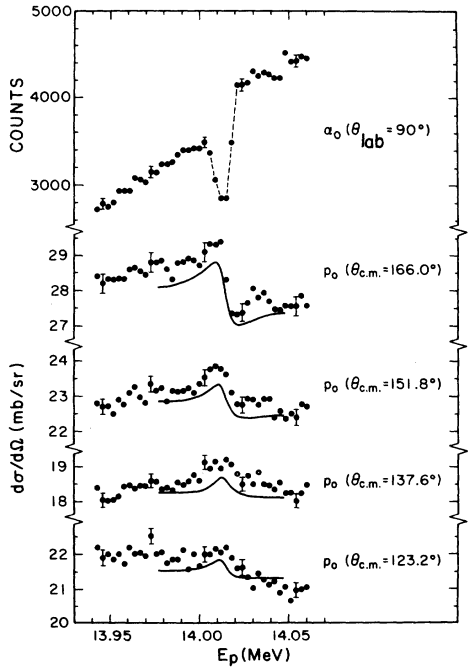

FIG. 9. ^{16}O(p,α)^{13}N data and phase-shift analysis of the ^{16}O(p,p)^{16}O elastic scattering data for the $T=\frac{3}{2}$ resonance at $E_p=14.02$ MeV. Sample relative error bars are shown. The dashed line with the (p,α) data is only to guide the eye.

Snover, and Paul[7] to observe this level as a resonance in the $^{16}O(p,\gamma)^{17}F$ reaction.

$E = 14.177/14.310$ MeV
($T = \frac{3}{2}$ fifth and sixth excited states)

The states are seen as prominent resonances in the elastic-scattering and reaction cross-section data presented in Figs. 11–14. A phase-shift analysis of the elastic scattering data using the procedures discussed above establishes $J^\pi = \frac{3}{2}^-$ for the level at $E_x = 14.177$ and $J^\pi = \frac{7}{2}^-$ for the level at 14.310 MeV. Comparisons of the resulting cross-section predictions with the experimental excitation functions are shown in Fig. 11. The resonance parameters for these two levels extracted by this analysis are listed in Table I.

These levels were previously located by Van Bree *et al.*[21]; their assignment of negative parity for both resonances and their suggestion of $l = 3$ for the upper resonance are consistent with our results. More recently Harakeh, Snover, and Paul[7] assigned $J^\pi = (\frac{3}{2}, \frac{5}{2}, \frac{7}{2})^-$ for both levels on the basis of their $^{16}O(p,\gamma)^{16}F$ data. The recent $^{11}B(^7Li,p)^{17}N$ assignments[8] of $(\frac{3}{2}, \frac{5}{2}, \frac{7}{2})$ and $(\frac{1}{2}^-, \frac{3}{2}^-)$ to the corresponding levels in ^{17}N are also consistent with the results of our analysis.

These results are all inconsistent with the recent suggestion[27] that $J^\pi = \frac{5}{2}^+$ for the resonance at $E_p = 14.579$ MeV. That suggestion was made on the basis of cross-section and polarization

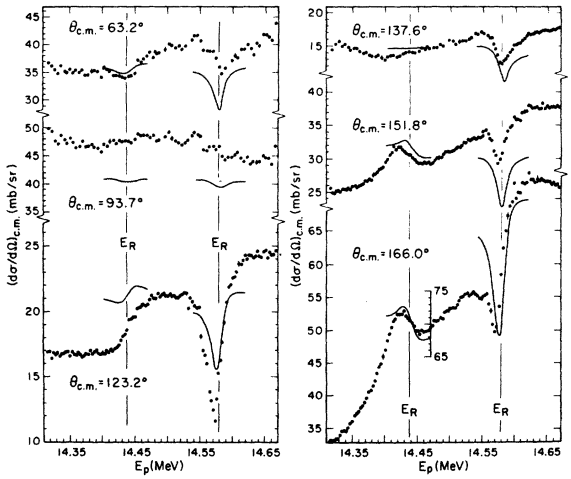

FIG. 11. Single-level phase-shift analyses of the ^{16}O-$(p,p)^{16}O$ elastic scattering data for the $T = \frac{3}{2}$ resonances at $E_p = 14.44$ and 14.58 MeV. Sample relative error bars are shown.

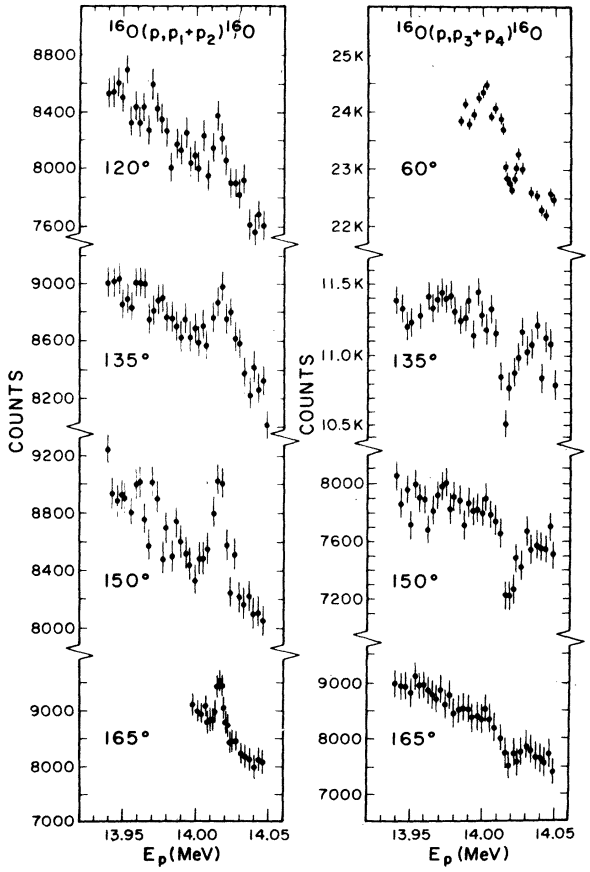

FIG. 10. $^{16}O(p,p')^{16}O$ inelastic scattering data at the $T = \frac{3}{2}$ resonance at $E_p = 14.02$ MeV. Sample relative error bars are shown.

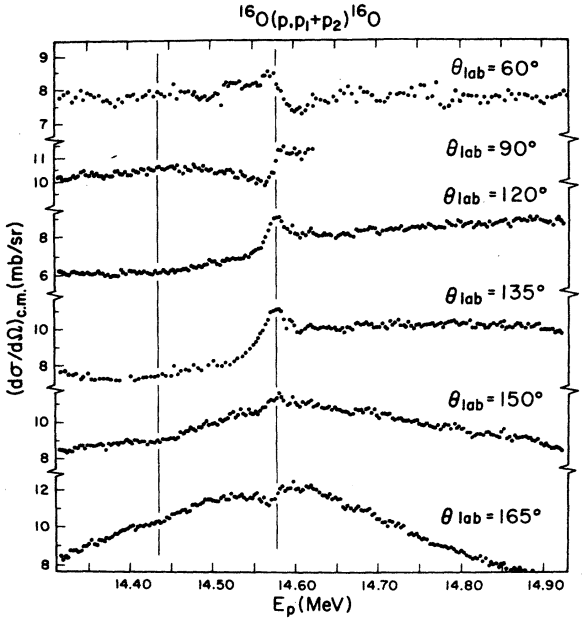

FIG. 12. $^{16}O(p,p')^{16}O$ inelastic scattering data in the region of the $T = \frac{3}{2}$ resonances at $E_p = 14.44$ and 14.58 MeV. The vertical lines indicate the locations of these resonances as determined from the analysis of the elastic scattering.

measurements at $\theta_{lab}=145$ and 165°. In Fig. 15 we have compared the $(d\sigma/d\Omega)$ predictions for a $\frac{5}{2}^+$ resonance and a $\frac{7}{2}^-$ resonance, and it is clear that although resonances for these two partial waves can be made to behave similarly at backward angles there are striking differences at forward angles. From a comparison of the curves in Fig. 15 with our data in Fig. 11, it is clear that our data at $\theta_{c.m.}=63.2$ and 93.7° definitely indicate a $\frac{7}{2}^-$ resonance rather than a $\frac{5}{2}^+$.

Higher $T=\frac{3}{2}$ excited states

The search for additional $T=\frac{3}{2}$ states in ^{17}F was extended in steps of 5 keV for another 2 MeV above the resonances at $E_p=14.44$ and 14.58 MeV to a proton energy of 16.60 MeV, $E_x=16.209$ MeV. The resulting elastic scattering excitation functions are plotted in Fig. 16 and show no obvious evidence for such states. The approximate expected locations for additional $T=\frac{3}{2}$ resonances (based on known $T=\frac{3}{2}$ levels in ^{17}N and ^{17}O) are indicated by the lines at the top of the plot. The two arrows indicate energies at which discontinuities in the experimental measurements were caused by instrumental effects, specifically a significant adjustment of the SCA windows and a substantial retuning of the beam-transport parameters.

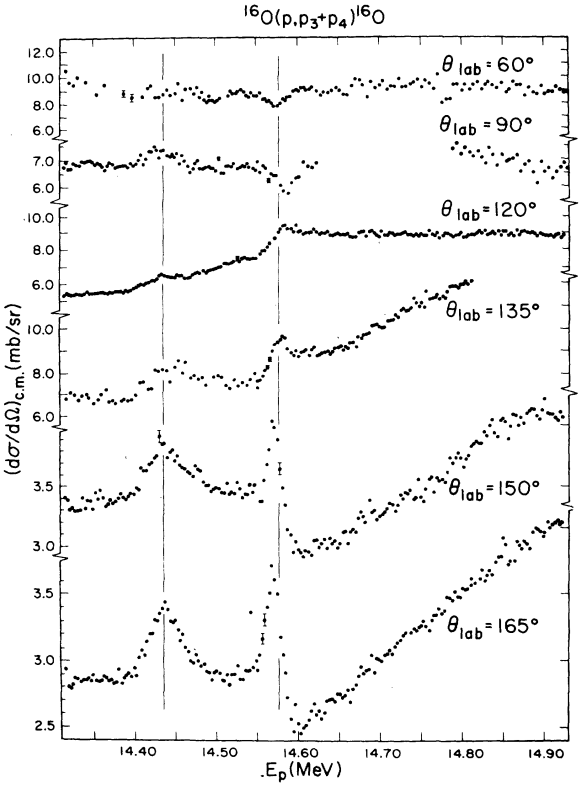

FIG. 13. ^{16}O$(p,p')^{16}$O inelastic scattering data in the region of the $T=\frac{3}{2}$ resonances at $E_p=14.44$ and 14.58 MeV. The vertical lines indicate the locations of these resonances as determined from the analysis of the elastic scattering. Sample relative error bars are shown.

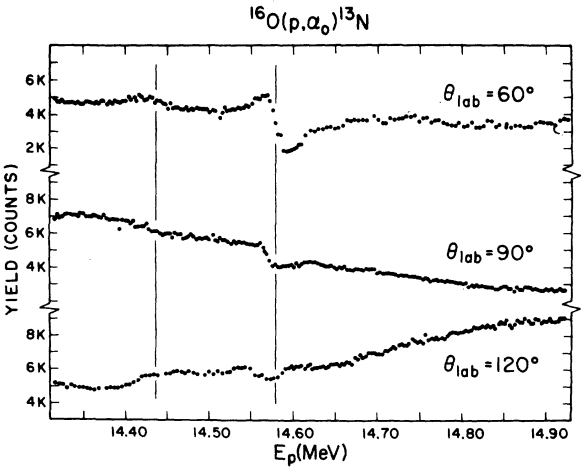

FIG. 14. ^{16}O$(p,\alpha)^{13}$N data in the region of the $T=\frac{3}{2}$ resonances at $E_p=14.44$ and 14.58 MeV. The vertical lines indicate the locations of these resonances as determined from the analysis of the elastic scattering.

V. DISCUSSION

A simple shell-model description of the low-lying, negative-parity states in ^{17}N can be ob-

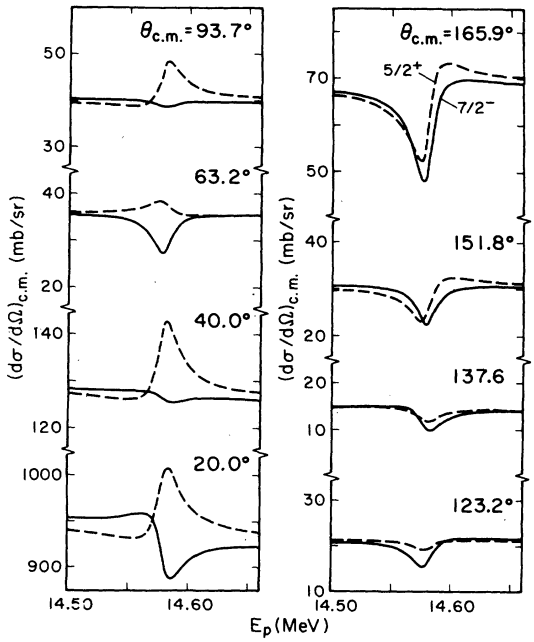

FIG. 15. Comparison of the predicted excitation functions for a $\frac{7}{2}^-$ and a $\frac{5}{2}^+$ resonance at $E_p=14.58$ MeV.

tained by coupling a $p_{1/2}$ proton hole to the low-lying states in ^{18}O, as suggested previously by Littlejohn[28] and by Margolis and deTakacsy.[29] In such a model the three lowest states in ^{18}O (0.00, 0^+; 1.98, 2^+; and 3.55, 4^+) are seen as predominantly $d_{5/2}{}^2$ neutron pairs outside a closed p-shell core. The excited 0^+ state at 3.63 MeV is an $s_{1/2}{}^2$ neutron pair, while an $s_{1/2}d_{5/2}$ neutron configuration can account for the 3.92-MeV (2^+) and the 5.37-MeV (3^+) levels in ^{18}O. Coupling a $p_{1/2}$ proton hole to the $d_{5/2}{}^2$ configurations would generate a set of $\frac{1}{2}^-$, $\frac{3}{2}^-$, $\frac{5}{2}^-$, $\frac{7}{2}^-$, and $\frac{9}{2}^-$ levels in ^{17}N. In fact, the results of the present $^{16}O+p$ phase-shift analysis and the Oxford ^{17}N results[8] establish the location of the first four of these levels, e.g. Fig. 17. Furthermore, the $^{11}B(^7Li,p)$-^{17}N work[8] also suggests the identification of the 3.63-MeV level in ^{17}N as the $\frac{9}{2}^-$ member of this configuration. The $T_z=-\frac{1}{2}$ analog of this level was not seen in the present $^{16}O+p$ experiments. The $\frac{3}{2}^-$ state at 3.20 MeV in ^{17}N and its $T_z=-\frac{1}{2}$ analog at $E_x=14.177$ MeV in ^{17}F can then be seen as corresponding to a $p_{1/2}$ hole coupled to the $(d_{5/2}s_{1/2})_{2^+}$ configuration.

The low-lying positive-parity states in ^{17}N must correspond instead to $(p_{1/2})^{-2}$ 3p-2h configurations. These states can be obtained either by coupling a second $p_{1/2}$ hole to the 3p-1h states in ^{18}O [$E_x=4.45$ MeV, $^{19}F(\frac{1}{2}^+)\otimes p_{1/2}{}^{-1}$, and $E_x=5.09$ MeV, $^{19}F(\frac{5}{2}^+)\otimes p_{1/2}{}^{-1}$] [30] or by removing an sd-shell proton from one of the 4p-2h configurations in ^{18}O (e.g. 0^+ at $E_x=5.33$ MeV).[31] Although these 3p-1h and 4p-2h states lie well above the 4^+, 2p-0h state at 3.55 MeV in ^{18}O, the corresponding 3p-2h states in ^{17}N would be expected to lie below the 2p-1h states based on the 3.55-MeV 4^+ state because it is energetically easier to remove the unpaired $p_{1/2}$ proton from the 3p-1h configuration or to remove one of the sd protons from the 4p-2h configuration than to remove one of the paired $p_{1/2}$ protons from the 2p-0h configuration. In fact, a comparison of the proton separation energies for various configurations in the $A=15$–18 region where one can identify the character of the separated proton indicates that relative to the (2p-0h) $\rightarrow$ (2p-1h) configuration, the (3p-1h) $\rightarrow$ (3p-2h) configurations will be lowered by 1 to 2 MeV and the

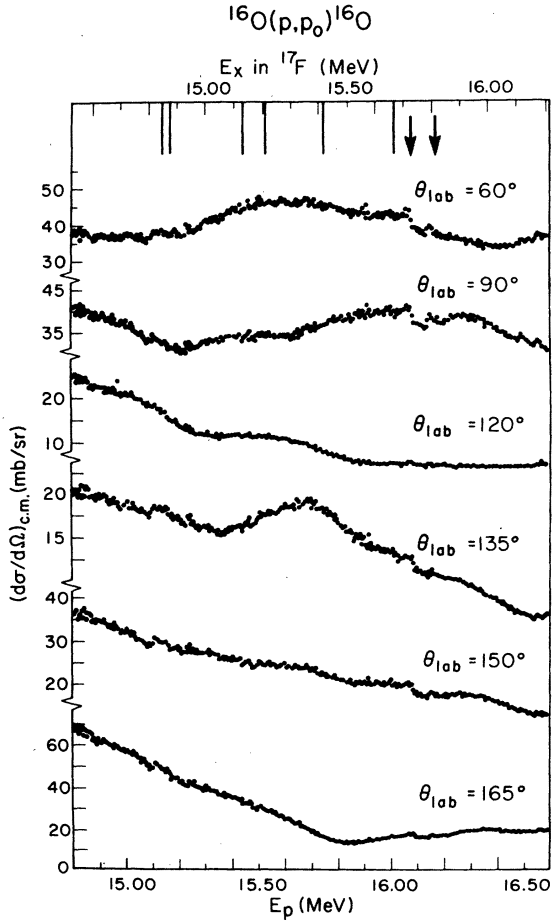

FIG. 16. $^{16}O(p,p)^{16}O$ elastic scattering excitation functions measured in 5-keV steps up to $E_p=16.60$ MeV. The vertical lines at the top of the figure indicate the expected location of additional $T=\frac{3}{2}$ states in ^{17}F on the basis of the excitation energies of states in ^{17}N. The two arrows indicate energies at which discontinuities in the experimental measurements were caused by instrumental effects.

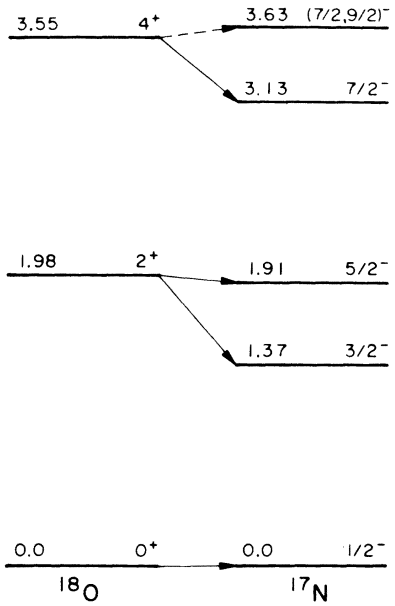

FIG. 17. The low-lying 2p-1h, $T=\frac{3}{2}$ negative-parity states in $A=17$ related via the coupling of a $p_{1/2}$ hole to the low-lying 2p-0h, $T=1$ states in $A=18$.

(4p-2h) – (3p-2h) configurations by ~2 to 3 MeV. (For example, the removal of an *sd*-shell proton from ^{18}Ne to form the lowest $\frac{1}{2}^+$ and $\frac{5}{2}^+$ states in ^{17}F costs about 2.8 MeV less than the removal of a paired $p_{1/2}$ proton to form the 3.11-MeV, $\frac{1}{2}^-$ excited state in ^{17}F.) This lowering of the expected location of the 3p-2h positive-parity states in ^{17}N is consistent with the observed location of the lowest positive-parity states in ^{17}N, $\frac{1}{2}^+$ at 1.85 MeV and $\frac{5}{2}^+$ at 2.53 MeV.

All of the $T=\frac{3}{2}$ states in ^{17}F above $E_x=12.728$ MeV are unbound to isospin-allowed decays, and a study of these decays can provide information about the configurations of these states. (An analysis of the various isospin-forbidden decays of these states gives us information only about the character of the $T=\frac{1}{2}$ impurities mixed into these states and *not* about the $T=\frac{3}{2}$ configurations.) Unfortunately, none of the isospin-allowed decays have been directly observed for these states. However, if we take the 0.5- to 3-keV widths of the four lowest $T=\frac{3}{2}$ states as an indication of the widths to be expected due to $T=\frac{1}{2}$ impurities (the lowest two are bound to isospin-allowed decays; the next two are unbound to the isospin-allowed, ^{15}N + 2p, decay by only ~300 keV so that their isospin-allowed decays will be greatly inhibited by the Coulomb barrier), then the considerably larger widths (12 to 27 keV) of the next three $T=\frac{3}{2}$ states in ^{17}F show the effects of the isospin-allowed decay channels. Furthermore, the relative sizes of these three widths are consistent with the configuration descriptions discussed above. Because the isospin-allowed decays are to [^{15}N + 2$p \cong$ (0p-1h) + 2p] and [^{16}O* ($T=1$) + $p \cong$ (1p-1h) + 1p] configurations, the decay of the $\frac{5}{2}^+$ (3p-2h) state ($\Gamma=12$ keV) would be expected to be weaker than the decays of the negative-parity (2p-1h) states ($\Gamma=20$ and 27 keV). Among the negative-parity states, the centrifugal barrier should inhibit the decay of the $\frac{7}{2}^-$ state ($\Gamma=20$ keV) relative to the decay of the $\frac{3}{2}^-$ state ($\Gamma=27$ keV). [The $\frac{3}{2}^-$ state can decay by *s*-wave proton emission to the lowest three ^{16}O ($T=1$) states (*d* wave to the fourth) and by emission of two *s*-wave protons to the ^{15}N ground state. The $\frac{7}{2}^-$ state, however, can decay to the first four $T=1$ states of ^{16}O only by *g*-, *d*-, *d*-, and *s*-wave proton emission, respectively, or to the ^{15}N ground state by emission of two *p*-wave protons (or one *d*-wave and one *s*-wave proton, etc.).]

An analysis of the masses of the various $T=\frac{3}{2}$ levels in the $A=17$ quartet in terms of the isobaric multiplet mass equation,

$$M(A, T_z) = a + bT_z + cT_z^2,$$

is presented in Table II. The parameters *a*, *b*, and *c* and their errors were determined from a weighted least-squares fit to the masses. For the cases where all four members of a quartet are known, the errors in the $T_z=-\frac{3}{2}$ members are too large to justify the inclusion of a cubic term. The ^{17}Ne excited state at 1.84 ± 0.07 MeV has not been included in this analysis; it is presumably the $T=-\frac{3}{2}$ projection of either the $\frac{1}{2}^+$ or $\frac{5}{2}^-$ member of the 1.86/1.91 MeV doublet in ^{17}N (or the unresolved analogs of both), but there is no information to indicate which. The ^{17}Ne (2.77-MeV) state and the two highest ^{17}O states listed in the table are enclosed in parentheses to indicate that since there is no spin-parity information available for these levels it is not clear that they are indeed the proper analogs of the ^{17}N and ^{17}F states listed on the same line. The ordering of the $\frac{7}{2}^-$, $\frac{3}{2}^-$ doublet is reversed in ^{17}N and ^{17}F, and in ^{17}O where these levels are only 60 keV apart the simple ordering of the levels is not sufficient to establish their correspondence to other members of the $T=\frac{3}{2}$ quartet. (A similar situation involving reversed ordering exists for the $\frac{1}{2}^+$, $\frac{5}{2}^-$ doublet at lower excitation energy, but in that case spin-parity information for the ^{17}O levels determines the correspondence.)

In examining the behavior of the coefficients *b*

TABLE II. $A=17$ $T=\frac{3}{2}$ quartet masses.

J^π	^{17}N($T_z=\frac{3}{2}$)	^{17}O($T_z=\frac{1}{2}$)	^{17}F($T_z=-\frac{1}{2}$)	^{17}Ne($T_z=-\frac{3}{2}$)	a (MeV)	b (MeV)	c (MeV)	χ^2
$\frac{1}{2}^-$	7.871 ± 0.015	10.272 ± 0.005	13.152 ± 0.007	16.479 ± 0.050	11.652 ± 0.005	−2.878 ± 0.008	0.237 ± 0.009	0.30
$\frac{3}{2}^-$	9.244 ± 0.015	11.658 ± 0.005	14.505 ± 0.005	17.829 ± 0.086	13.027 ± 0.005	−2.848 ± 0.007	0.218 ± 0.009	0.24
$\frac{1}{2}^+$	9.721 ± 0.015	12.140 ± 0.006	15.032 ± 0.005	···	13.527 ± 0.005	−2.892 ± 0.008	0.237 ± 0.010	
$\frac{5}{2}^-$	9.778 ± 0.015	12.186 ± 0.006	15.015 ± 0.004	···	13.548 ± 0.005	−2.829 ± 0.007	0.211 ± 0.010	
$\frac{5}{2}^+$	10.398 ± 0.015	12.833 ± 0.005	15.734 ± 0.004	(19.249 ± 0.086)	14.224 ± 0.004	−2.903 ± 0.006	0.237 ± 0.009	2.74
$\frac{7}{2}^-$	11.000 ± 0.015	(13.475 ± 0.012)	16.262 ± 0.006	···	14.829 ± 0.009	−2.787 ± 0.013	0.156 ± 0.014	
$\frac{3}{2}^-$	11.079 ± 0.015	(13.412 ± 0.008)	16.129 ± 0.006	···	14.723 ± 0.007	−2.717 ± 0.010	0.192 ± 0.011	

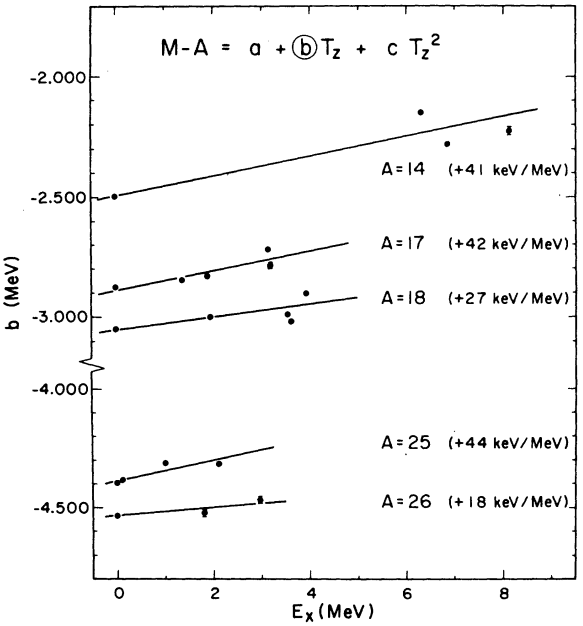

FIG. 18. Dependence of the linear coefficient in the isobaric multiplet mass equation on the excitation energy of the multiplet. The straight lines through the data points are least-squares fits and have the slope indicated for each mass. Error bars determined from fitting the individual multiplets are shown except where they are smaller than the plotted points.

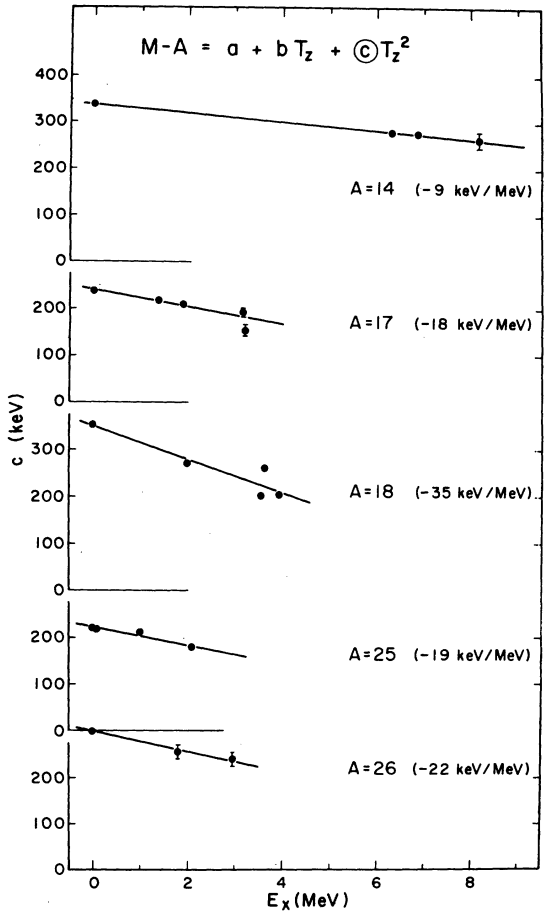

FIG. 19. Dependence of the quadratic coefficient in the isobaric multiplet mass equation on the excitation energy of the multiplet. The straight lines through the data points are least-squares fits and have the slope indicated for each mass. Error bars determined from fitting the individual multiplets are shown except where they are smaller than the plotted points.

and c in Table II, there is a suggestion that b is more negative for the positive-parity states than for the negative-parity ones while c is more positive for the positive-parity states than for the negative-parity ones. From an examination of the dependence of these coefficients on A (e.g. Jänecke[32]), it might be argued that such behavior is expected for b on the basis that the negative-parity states with an odd hole in the p shell should behave more like the p-shell quartets than the positive-parity states which have an odd particle in the sd shell. However, such an argument is in disagreement with the apparent variation of c between positive- and negative-parity states.

There is also a suggestion in Table II that both the b and the c coefficients for the negative-parity states are functions of excitation energy

$$\Delta b/\Delta E_x \approx +42 \text{ keV/MeV},$$

$$\Delta c/\Delta E_x \approx -18 \text{ keV/MeV}.$$

An analysis of the data of Benenson *et al.*[1] on the $A=25$, $T=\frac{3}{2}$ quartet also suggests a similar energy dependence of the b and c coefficients for the four lowest positive-parity states ($\Delta b/\Delta E_x \sim +50$ keV/MeV and $\Delta c/\Delta E_x \sim -15$ keV/MeV). In examining the $T=1$ triplets in $A=14$ ($0 \leq E_x \leq 8.5$ MeV),[33] $A=18$ ($0 \leq E_x \leq 4$ MeV),[34] and $A=26$ ($0 \leq E_x \leq 3$ MeV)[35] (virtually the only other isospin multiplets for which more than one or two excited states are well identified and spread over an energy range of more than 2 MeV) the data are also consistent with energy-dependent terms of this same sign and magnitude, as seen in Figs. 18 and 19. The energy dependence of these coefficients has been examined in terms of the Thomas-Ehrman shift and in terms of variations in the nuclear charge distribution. The results of this analysis will be presented separately.[36]

VI. ACKNOWLEDGMENTS

The authors would like to thank Dr. M. J. Fritts, Dr. W. B. Thompson, M. E. Cobern, and D. J.

Pisano for many hours of assistance in the carrying out of these measurements. We gratefully acknowledge the generosity of Dr. M. J. LeVine and Dr. W. B. Thompson in making available to us several of their computer codes. We are also happy to thank Dr. Rod Hiddleston for helpful discussions concerning his polarization work and optical-model analyses, to thank Dr. K. Snover and Dr. P. Paul for helpful discussions concerning the use of complex phase shifts in the collision matrix, and to thank Dr. David Rogers for sending us the Oxford ^{17}N results prior to publication.

---

†Work supported under U.S. Atomic Energy Commission Contract No. AT(11-1)-3074.

*Present address: Stein Associates, 1380 Main Street, Walthan, Massachusetts 02154.

[1]e.g. W. Benenson, J. Driesbach, I. D. Proctor, G. F. Trentelman, and B. M. Preedom, Phys. Rev. C 5, 1426 (1972).

[2]F. Ajzenberg-Selove, Nucl. Phys. A166, 1 (1971).

[3]R. Mendelson, J. M. Loiseaux, G. Wozniak, and J. Cerny, private communication as quoted in Ref. 2.

[4]M. J. LeVine and P. D. Parker, Phys. Rev. 186, 1021 (1969).

[5]D. Hartwig, KFK-1426 (June 1971).

[6]A. B. McDonald, T. K. Alexander, O. Hausser, and D. L. Disdier, Bull. Am. Phys. Soc. 16, 489 (1971); and private communication.

[7]M. H. Harakeh, K. A. Snover, and P. Paul, Bull. Am. Phys. Soc. 17, 98, 442 (1972); and private communication.

[8]J. A. Becker, T. K. Alexander, A. Anyas-Weiss, T. A. Belote, S. P. Dolan, N. A. Jelley, W. L. Randolph, and D. W. O. Rogers, Bull. Am. Phys. Soc. 18, 79 (1973); and D. W. O. Rogers, private communication (to be published).

[9]J. C. Overley, P. D. Parker, and D. A. Bromley, Nucl. Instrum. Methods 68, 61 (1969).

[10]Hamilton Precision Metals, Lancaster, Pennsylvania.

[11]e.g. C. Detraz, J. Cerny, and R. H. Pehl, Phys. Rev. Lett. 14, 708 (1965).

[12]C. L. Critchfield and D. C. Dodder, Phys. Rev. 76, 602 (1949).

[13]R. H. Siemssen, private communication.

[14]B. A. Watson, P. P. Singh, and R. E. Segal, Phys. Rev. 182, 977 (1969).

[15]C. B. Duke, Phys. Rev. 129, 681 (1963).

[16]G. Hardie, R. L. Dangle, and L. D. Oppliger, Phys. Rev. 129, 353 (1963).

[17]S. R. Salisbury, G. Hardie, L. Oppliger, and R. Dangle, Phys. Rev. 126, 2143 (1962).

[18]J. C. Hardy, J. E. Esterl, R. G. Sextro, and J. Cerny, Phys. Rev. C 3, 700 (1971).

[19]J. C. Hardy, J. E. Esterl, R. G. Sextro, and J. Cerny, in *Nuclear Isospin*, edited by J. D. Anderson, S. D. Bloom, J. Cerny, and W. W. True (Academic, New York, 1969), p. 725.

[20]J. R. Patterson, H. Winkler, and C. S. Zaidins, Phys. Rev. 163, 1051 (1967).

[21]R. G. Van Bree, Ph.D. thesis, Rutgers University, 1968 (unpublished); and G. M. Temmer, B. Teitelman, R. G. Van Bree, and H. Ogata, J. Phys. Soc. Jap. Suppl. 24, 299 (1968).

[22]J. C. Hardy, D. J. Skyrme, and P. S. Fisher, P.L.A. Progress Report No. RHEL/R136, Rutherford Laboratory, 1966 (unpublished), and P.L.A. Progress Report No. RHEL/R156, Rutherford Laboratory, 1967 (unpublished).

[23]I. D. Procter, W. Benenson, and D. L. Bayer, Bull. Am. Phys. Soc. 17, 442 (1972).

[24]E. G. Adelberger and C. A. Barnes, Phys. Lett. 23, 474 (1966).

[25]E. G. Adelberger, A. B. McDonald, and C. A. Barnes, Nucl. Phys. A124, 49 (1969).

[26]C. Dêtraz and H. H. Duhm, Phys. Lett. 29B, 29 (1969).

[27]J. G. Cramer, M. Hasinoff, E. Preikschat, G. W. Roth, and W. G. Weitkamp, Bull. Am. Phys. Soc. 16, 829 (1971); N.P.L. Annual Report, University of Washington, 1972 (unpublished); and private communication.

[28]C. S. Littlejohn, Phys. Rev. 114, 250 (1959).

[29]B. Margolis and N. deTakacsy, Can. J. Phys. 44, 1431 (1966).

[30]A. P. Zucker, Phys. Rev. Lett. 23, 983 (1969).

[31]W. H. Bassichis, B. Giraud, and G. Ripka, Phys. Rev. Lett. 15, 980 (1965).

[32]J. Jänecke, in *Isospin in Nuclear Physics*, edited by D. H. Wilkinson (North-Holland, Amsterdam, 1969), p. 297.

[33]F. Ajzenberg-Selove, Nucl. Phys. A152, 1 (1970).

[34]F. Ajzenberg-Selove, Nucl. Phys. A190, 1 (1972).

[35]P. M. Endt and C. Van der Leun, Nucl. Phys. A105, 1 (1967).

[36]P. D. Parker and C. M. Baglin, to be published.